

## Article

# Green Synthesis of Silver Nanoparticles Using *Bellevalia Flexuosa* Leaves Extract

Nusaiba Al-Nemrawi <sup>1,\*</sup> , Fatima Hameedat <sup>1</sup>  and Tamam El-Elimat <sup>2</sup>

<sup>1</sup> Department of Pharmaceutical Technology, Faculty of Pharmacy, Jordan University of Science and Technology, Irbid 22110, Jordan

<sup>2</sup> Department of Medicinal Chemistry and Pharmacognosy, Faculty of Pharmacy, Jordan University of Science and Technology, Irbid 22110, Jordan

\* Correspondence: nknemrawi@just.edu.jo

**Abstract:** Silver nanoparticles (AgNPs) have broad biocidal activities, and are widely employed as an active ingredient in antiseptic, anti-viral, and anti-inflammatory preparations. Green-synthesizing AgNPs would be a rapid, cheap, and environmentally friendly method of synthesis. The methanolic extract of the leaves of *Bellevalia flexuosa* Boiss. (Asparagaceae) was used for the green synthesis of the AgNPs. The effects of the pH and the concentration of silver nitrate (AgNO<sub>3</sub>) on the synthesis of the AgNPs were investigated. The AgNPs produced above pH 10, and 1 mM of AgNO<sub>3</sub> resulted in lower hydrodynamic diameters. Ultraviolet-visible spectroscopy, Fourier-transform infrared spectroscopy, and X-ray diffraction proved the formation of the AgNPs, with a face-centered, cubed geometry. Scanning electron microscopy images showed colloidal and well-dispersed nanoparticles. In addition, the antibacterial activities of the prepared AgNPs were assessed by optical densities (ODs) against Gram-positive bacteria (*Enterococcus faecalis* and *Staphylococcus epidermidis*) and Gram-negative bacteria (*Pseudomonas aeruginosa*, *Escherichia coli*, *Klebsiella pneumoniae*, and *Salmonella enterica*). The broths of Gram-negative and Gram-positive bacteria that contained AgNPs, showed lower OD values compared to the controls. In conclusion, AgNPs were prepared using *B. flexuosa* methanolic extract, and showed antibacterial activity against the tested bacterial strains.

**Keywords:** silver nanoparticles; green synthesis; *bellevalia flexuosa*; green nanoparticles; antimicrobial activity



**Citation:** Al-Nemrawi, N.; Hameedat, F.; El-Elimat, T. Green Synthesis of Silver Nanoparticles Using *Bellevalia Flexuosa* Leaves Extract. *Sci. Pharm.* **2022**, *90*, 60. <https://doi.org/10.3390/scipharm90040060>

Academic Editor: Murali Mohan Yallapu

Received: 20 August 2022

Accepted: 23 September 2022

Published: 6 October 2022

**Publisher's Note:** MDPI stays neutral with regard to jurisdictional claims in published maps and institutional affiliations.



**Copyright:** © 2022 by the authors. Licensee MDPI, Basel, Switzerland. This article is an open access article distributed under the terms and conditions of the Creative Commons Attribution (CC BY) license (<https://creativecommons.org/licenses/by/4.0/>).

## 1. Introduction

Metallic nanoparticles (NPs) are metals within the size range of 1–1000 nm. Nanosize particles have different characteristics when compared to their bulk counterparts, in terms of stability, and electronic, optical, and chemical characteristics [1]. They have a wide range of applications, including biotechnology, and as vehicles for gene and drug delivery. In addition, they have the potential to be used as catalysts, and in site-specific targeting [2]. Such nanomaterials can be prepared and modified with various techniques, and used directly or as adjuvant with other drugs. Among these NPs are silver NPs (AgNPs), which are nowadays attracting attention because of their antiseptic properties [3–5]. AgNPs have properties that enable them to kill Gram-negative and Gram-positive bacteria [6]. They can disturb the enzymatic activities of microorganisms by disrupting their unicellular membrane [7]. Their mechanism of action involves the inactivation of the respiratory chain, and the disruption of the cell membrane, to leak their cellular contents. They can bind to the functional group of proteins leading to protein denaturation and cell death, block DNA replication, and denature enzymes that transport nutrients across the bacterial cell membrane [8]. With their broad biocidal activities, therefore, AgNPs are widely employed as an active ingredient in antiseptic, antiviral, antifungal, and anti-inflammatory preparations. AgNPs have been added to wound dressings, topical creams, antiseptic sprays, and fabrics [9]. In addition, AgNPs are used in food storage containers [10]. They

are also employed in coating the surfaces of medical devices, bandages, footwear, and countless household items, to reduce nosocomial infections [11]. Recently, the major focus on using AgNPs has been as a disinfectant during the COVID-19 pandemic, to control possible indoor airborne infections [12].

Various methods are available for manufacturing NPs, including chemical [13], photochemical [14], radiation [15], Langmuir–Blodgett [16], microwave [17], laser [18], and biological techniques [19,20]. Most chemical methods, however, involve the use of toxic and hazardous materials in the environment. The fabrication of NPs using microorganisms or plant extracts is referred to as ‘green nanotechnology’ [21]. The first record of green synthesis, using alfalfa, was in 2003; since that time, the production of NPs has increased [22]. Green synthesis of NPs is rapid, cheap, easy, and environmentally friendly [23]. Biologically, it has been proven that the cellular intake and internalization of green NPs depends on the concentration of the NPs. In addition, it has been suggested that AgNPs directly diffuse into cells, or internalize via receptor-mediated endocytosis [24].

A large number of plants have been investigated for green synthesis of AgNPs, and have been applied in various fields, such as catalysis, biosensing, imaging, drug delivery nanodevice fabrication, and medicine [21]. The key phytochemicals—as identified in IR spectroscopic data—responsible for converting silver ions into AgNPs are terpenoids, glycosides, alkaloids, and phenolics (flavonoids, coumarins, ubiquinones, tannins, etc.) [25,26].

*Bellevalia flexuosa* Boiss. (Asparagaceae) is a perennial wild-growing herb in Jordan, known locally as ‘Drooping Onion’ [27]. Chemical investigation of the bulbs of *B. flexuosa* resulted in the isolation of a set of homoisoflavonoids [28]. Homoisoflavonoids are a rare subclass of flavonoids that possess a wide range of biological activities, including antioxidant, anti-inflammatory, cytotoxic, and antimicrobial activities [29]. Hence, *B. flexuosa* could be a good candidate for the green synthesis of AgNPs.

The present study was therefore carried out, to examine the use of dried *B. flexuosa* leaves in the form of a methanolic extract to prepare AgNPs, and to investigate the effect of several variables on the preparation of these NPs. The prepared NPs were characterized and evaluated for their stability and efficacy as antibacterial agents.

## 2. Materials and Methods

### 2.1. Materials

Leaves of *B. flexuosa* were collected from the campus of the Jordan University of Science and Technology (JUST), Irbid, Jordan. A voucher specimen (PHS-122) was deposited in the herbarium of the Faculty of Pharmacy, JUST. Silver nitrate (AgNO<sub>3</sub>), ammonia solution, and sodium hydroxide (NaOH) were purchased from Merck Chemical Co. (Darmstadt, Germany). *Enterococcus faecalis* (ATCC 29212), *Staphylococcus epidermidis* (ATCC 12228), *Pseudomonas aeruginosa* (ATCC 9027), *Escherichia coli* (ATCC 2452), *Klebsiella pneumoniae* (ATCC 1705), and *Salmonella enterica* (ATCC 103799) were purchased from Becton Dickinson and Company (Cockeysville, MD, USA). Mueller Hinton Broth II was purchased from MHB Biocorp (Warsaw, Poland). All other chemicals and solvents used in this work were of chemical grade.

### 2.2. Preparation of *B. flexuosa* Methanolic Extract

Air-dried leaves of *B. flexuosa* were ground to a powder, using a laboratory mill. The powdered leaves were defatted with hexane, using the Soxhlet apparatus, followed by exhaustive extraction with methanol at 60 °C. The solvent was evaporated under reduced pressure, to furnish the MeOH extract. A stock solution of the extract was prepared at a concentration of 8%, using distilled water.

### 2.3. Green Synthesis of Silver Nanoparticles (AgNPs)

The procedure for the preparation of the AgNPs was adapted from the literature, with some modifications [30]. Briefly, AgNO<sub>3</sub> solution was added dropwise to the stock solution of *B. flexuosa* in a ratio of 1:1, followed by adding 1 mL of ammonia, and then mixed gently

at different pH. An immediate change was noticed in the color of the solutions, which became dark green. The solutions were kept under continuous shaking in a water bath for 4 h at 45 °C and 100 rpm. The color of the mixture changed again from dark green to darker brown. After optimizing the pH, different concentrations of AgNO<sub>3</sub> (1, 5, and 10 mM) were used to prepare the NPs. Figure 1 is a scheme that explains the green synthesis of the AgNPs.

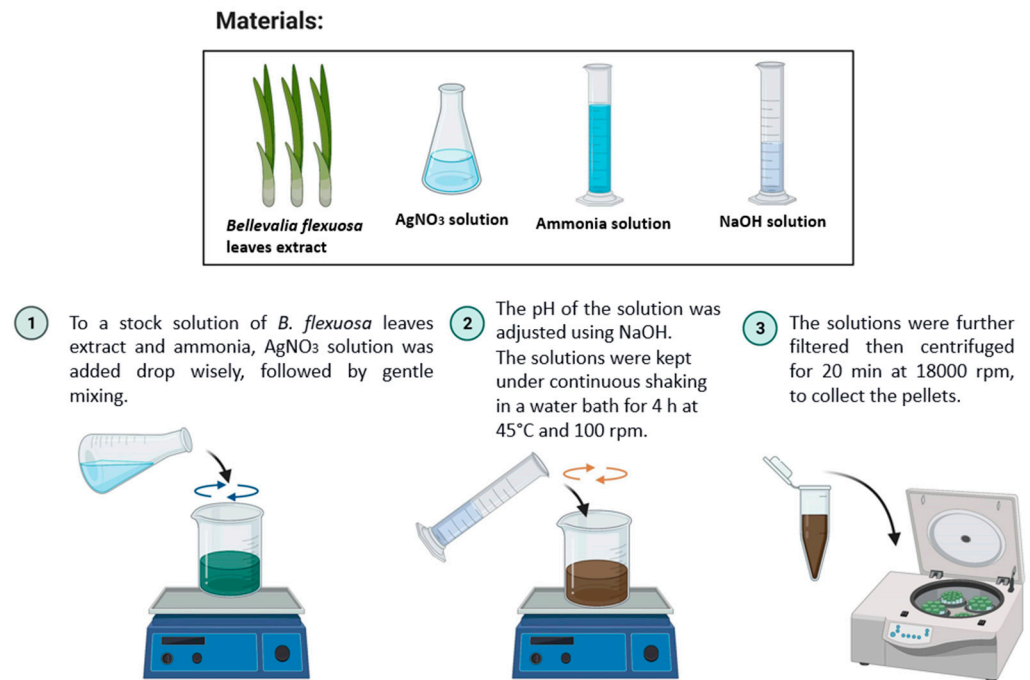


**Figure 1.** Scheme of the general method used in this work to synthesize green AgNPs. The materials used were *B. flexuosa* leaves extract and AgNO<sub>3</sub>, ammonia and NaOH solutions: 1. AgNO<sub>3</sub> solution was added, dropwise, to a stock solution of *B. flexuosa* leaves extract and ammonia, followed by gentle mixing; 2. The pH of the solution was adjusted, using NaOH. The solutions were kept under continuous shaking in a water bath for 4 h at 45 °C and 100 rpm; 3. The solutions were further filtered, then centrifuged for 20 min at 18,000 rpm.

The samples were then filtered three times, using a filter syringe of 0.45 µm pore size. The filtered solutions were then centrifuged for 20 min at 18,000 rpm. The precipitated pellets were washed three times with distilled water, followed by centrifugation for 5 min at 18,000 rpm. The precipitate was immediately freeze-dried, to obtain AgNPs as a dry powder. The powder was kept in a well-closed container until further investigation.

#### 2.4. Characterization of the Green-Synthesized AgNPs

The formation of the AgNPs was confirmed by an ultraviolet–visible (UV-Vis) spectrophotometer (EMC-61PC-UV, UK). The blank, Milli-Q water, and the solutions of AgNPs were filled in quartz cuvettes, and placed between a light source and a photodetector, to measure the intensity of a beam of light.

The hydrodynamic diameters, polydispersity index (PdI), and zeta potential (ZP) of the nanoparticles were measured, using a Zetasizer Nano ZS90 instrument (Malvern, Worcestershire, UK). The hydrodynamic diameters and PdI were determined at 25 °C, using dynamic light scattering. The ZP was calculated from the electrophoretic mobility of the NPs, using the Helmholtz–Smoluchowski equation, under an electrical field of 40 V/cm. All measurements were carried out in triplicate (n = 3).

Fourier-transform infrared spectroscopy (FT-IR) (Shimadzu, Kyoto, Japan) was used to evaluate the functional groups of the formed AgNPs. The FT-IR was provided with a high-performance diamond single-bounce attenuated total reflection (ATR) accessory that

covered a wavelength in the range of 400–4000  $\text{cm}^{-1}$ , had a resolution of 4  $\text{cm}^{-1}$ , and ran 64 scans per spectrum.

The determination of the X-ray diffraction (XRD) patterns of the AgNPs was recorded by an Ultima IV X-ray diffractometer (Rigaku, Tokyo, Japan) using cobalt radiation ( $\text{CuK}\alpha$ ), with a voltage of 40 kV and a current of 30 mA at room temperature. Diffraction angles of  $2\theta$ , starting from  $0^\circ$  to  $80^\circ$ , were used to analyze the powdered samples, which were placed on the sample holder on the X-ray diffractometer, and analyzed.

The morphology of the AgNPs was determined by scanning electron microscope (SEM) (Model QUANTA FEG 450, FEI, Thermo Fisher Scientific, Bremen, Germany).

The configuration of the AgNPs was determined by XRD spectra derived by Ultima IV X-ray diffractometer (Rigaku, Tokyo, Japan), using cobalt radiation ( $\text{CuK}\alpha$ ), with a voltage of 40 kV and a current of 30 mA at  $25^\circ\text{C}$ . Diffraction angles from  $0^\circ$  to  $60^\circ$  ( $2\theta$ ) were used. Powders were dispersed on a quartz sample holder, placed on a Goniometer, and diffracted using a DTEX detector.

### 2.5. Antibacterial Susceptibility Test

The antimicrobial activity of the AgNPs was evaluated using six bacterial strains. Two of the bacterial strains were Gram-positive: *Enterococcus faecalis* (ATCC 29212) and *Staphylococcus epidermidis* (ATCC 12228). Four of the bacterial strains were Gram-negative: *Pseudomonas aeruginosa* (ATCC 9027); *Escherichia coli* (ATCC 2452); *Klebsiella pneumoniae* (ATCC 1705); and *Salmonella enterica* (ATCC 103799). The microorganisms were cultured in a Mueller Hinton Broth II overnight at  $37^\circ\text{C}$ .

The AgNPs were dispersed in distilled water, with a concentration of 150  $\mu\text{g}/\text{mL}$ , and added to the bacterial test tubes. The quantification of the total number of bacteria was done in triplicate, where aliquots of suspension were analyzed with a spectrophotometer (Visible spectrophotometer V-1200, VWR, Radnor, PA, USA). The optical density (OD) was reported as bacterial proliferation expressed in a colony-forming unit (CFU/mL) ( $1 \text{ OD}_{600} = 1.5 \times 10^8 \text{ CFU}/\text{mL}$ ), and compared to the control broth [31].

## 3. Results and Discussion

### 3.1. Characterization of the AgNPs

The reduction of  $\text{AgNO}_3$  was the main step in the AgNPs synthesis that was affected by different parameters during the experimental procedure. The reaction time, however, was kept at 4 h, which had been optimized previously in the literature [32]. The concentration of the  $\text{AgNO}_3$ , on the other hand, was fixed at 1 mM, to study the effect of the pH on the synthesis of the AgNPs in the range of 3 to 11, which was optimized afterwards. The particles formed were characterized using a UV-Vis spectrophotometer, and the results obtained are shown in Figure 2.

The figure shows that the synthesis of the AgNPs was achieved at pH values of more than 10, which is indicated by the optical absorption band peak at around 430 nm. Absorption at 430 nm is considered the typical absorption for metallic AgNPs, due to the surface plasmon resonance [33]. Furthermore, the peak clearly became higher and narrower as the pH increased [34,35]. This indicated that increasing the pH enhanced the stability of the NPs formed, as reported previously in the literature [36]; therefore, pH 11 was chosen for further investigation. The weak absorption peak around 260 nm was explained by the presence of several organic compounds, which are known to interact with silver ions, and which suggest a possible mechanism for the reduction of the metal ions present in the solution [33,37]. Similar results obtained for green-synthesized AgNPs in the presence of *Artemisia herba-alba* extract at pH 12, with absorption peak of an average of 395 nm, were explained as an indication of well-dispersed NPs [38].

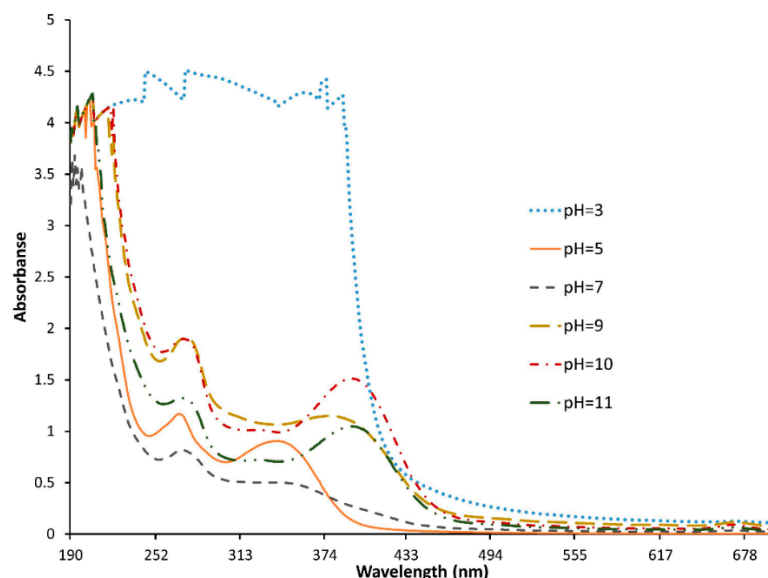


**Figure 2.** UV-Vis spectrophotometer of AgNPs prepared at different pH values, in the range of 3 to 11, synthesized from *B. flexuosa* leave extract, in the range of 190–700 nm, using ultraviolet-visible (UV-Vis) spectrophotometer (EMC-61PC-UV, Duisburg, Germany).

Afterwards, the pH was fixed at 11, to study the effect of the  $\text{AgNO}_3$  concentration. The UV-Vis spectra showed no difference between the three molarities tested: the same peak appeared at 396 nm, which meant that the NPs were formed successfully at the three pHs. However, differences in the hydrodynamic diameter and the ZP of the formed NPs were observed, as shown in Table 1. The lowest tested concentration (1 mM) showed the smallest NPs, the lowest charge in negative, and the lowest PDI. As the molarity increased from 1 to 10 mM, the hydrodynamic diameters of the particles increased, and the samples became more polydispersed. Likewise, the synthesized AgNPs using the leaf extract of *Peumus boldus* at different concentrations of  $\text{AgNO}_3$  (0.1 mM, 1 mM, 2 mM, 10 mM) showed an increase in the average hydrodynamic diameter of the AgNPs (ranging from 147 nm to 503 nm) [39]. In addition, the ZP of the AgNPs was affected by the concentration of  $\text{AgNO}_3$ , and showed instability in the high concentration of  $\text{AgNO}_3$  with  $-6$  mV. By contrast, at lower concentrations (1 mM and 5 mM) the ZP was higher in the negative ( $-27$  mV and  $-36$  mV, respectively) [40]. In general, the AgNPs carried a negative charge that was around  $-30$  mV, as mentioned by other research teams [41,42]. The ZP of metallic NPs is very important in determining the stability of the dispersion, where ZP of more than 25 mV and lower than  $-25$  mV is usually used to indicate good stability of NPs due to electrostatic repulsion [40].

**Table 1.** Hydrodynamic diameters, zeta potential (ZP), and polydispersity index (PDI) of AgNPs prepared using different concentrations of  $\text{AgNO}_3$  (1, 5, and 10 mM), and synthesized using *B. flexuosa* leave extract.

Property	AgNO <sub>3</sub> Concentration		
	1 mM	5 mM	10 mM
Hydrodynamic diameter (nm)	86.5 ± 1.8	352.9 ± 795.2	1219.0 ± 339.3
PdI	0.45 ± 0.0	0.93 ± 0.0	0.81 ± 0.1
ZP (mV)	-27 ± 0.3	-36 ± 3.6	-6 ± 3.5

Additionally, the uniformity of the NPs, indicated by the PDI (with values lower than 0.5), is crucial in any pharmaceutical industry, to assure efficacy, safety, and stability [43]. For instance, it was reported that heterogeneity enhances sedimentation of particles [44]. Moreover, the distribution of the particles affects the drug-release kinetics, which in turn

affects the drug bioavailability [45]. Other formulary and pharmacokinetic concerns were found to be related to the size distribution of the system.

The residuals of the biomolecules on the surface of the synthesized AgNPs were investigated, using FTIR spectroscopy. The results were compared for any critical shifts in functional peaks. Figure 3 compares the FTIR spectra of both the *B. flexuosa* MeOH extract and the synthesized AgNPs. In addition, Table 2 presents the main FTIR frequencies of the AgNPs spectrum. In the spectrum of the AgNPs, the sharp peaks around 3373, 2920 and 2850, and 1078  $\text{cm}^{-1}$  were ascribed to hydroxyl (OH), alkyl (–CH), and alcohol (C–O), respectively. As similar peaks with small shifts, intensity, and shape could be noticed in the extract spectrum, then the synthesized AgNPs may have contained natural compounds from the extract. However, the small shifts in the range of 2351–3396  $\text{cm}^{-1}$  in the *B. flexuosa* extract band, along with the formation of the carbonyl (C=O) band at 1743  $\text{cm}^{-1}$ , and the double bond at 1543 and 1575  $\text{cm}^{-1}$ , indicate the bioreduction of Ag and the stabilization of the formed AgNPs [46]. It was previously reported by Kumar et al. that the phenolic functional groups which appeared at 1637 and 3396  $\text{cm}^{-1}$  were responsible for the formation of AgNPs [41]. Therefore, the polyphenolic groups revealed at 1419, 1641, and 3373  $\text{cm}^{-1}$  in *B. flexuosa* MeOH extract were considered a suitable source for the bioreducing agents that helped in reducing the cationic Ag ( $\text{Ag}^+$ ) to metallic Ag ( $\text{Ag}^0$ ), as noted above [47].

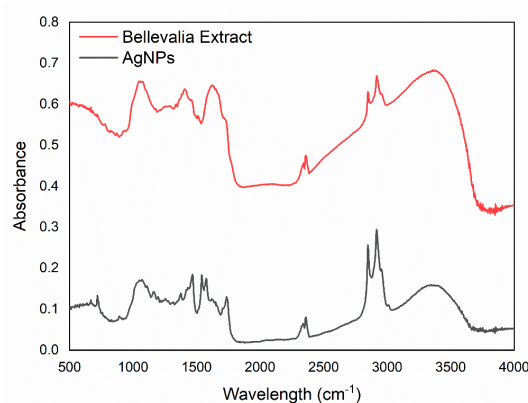


**Figure 3.** The FTIR spectra of both *B. flexuosa* methanolic extract and the synthesized AgNPs in the range of 400–4000  $\text{cm}^{-1}$ , with a resolution of 4  $\text{cm}^{-1}$ , and using FTIR (Shimadzu, Kyoto, Japan).

**Table 2.** FTIR spectral characteristics of AgNPs synthesized by *B. flexuosa* extract.

No.	IR Value	Functional Group Detection	Remark
1	719 $\text{cm}^{-1}$	–CH	–CH aromatic bending
2	902 $\text{cm}^{-1}$	–OH	–OH bending of carboxylic
3	1078, 1170 $\text{cm}^{-1}$	C–O or –C–O–C–	C–O stretching
4	1380 $\text{cm}^{-1}$	–CH	C–H bending of alkane
5	1471 $\text{cm}^{-1}$	–CH	C–H bending of alkane
6	1543, 1575 $\text{cm}^{-1}$	–C=C–	–C=C– stretching vibration
7	1743 $\text{cm}^{-1}$	C=O	C=O stretching of carbonyl
8	2850, 2920 $\text{cm}^{-1}$	–CH	–CH stretching of alkyl
9	3373 $\text{cm}^{-1}$	–OH	–OH stretching of alcohol/phenol

The XRD spectrum of the synthesized AgNPs is shown in Figure 4. The four major peaks, at 37.48°, 43.92°, 65.98°, and 77.08°, corresponded to the (111), (200), (220), and (311) reflection planes, respectively, of the face-centered cubed geometry [48,49]. A sharp peak around 55 (noted by +) may have been related to other crystalline compounds in the extract [50].

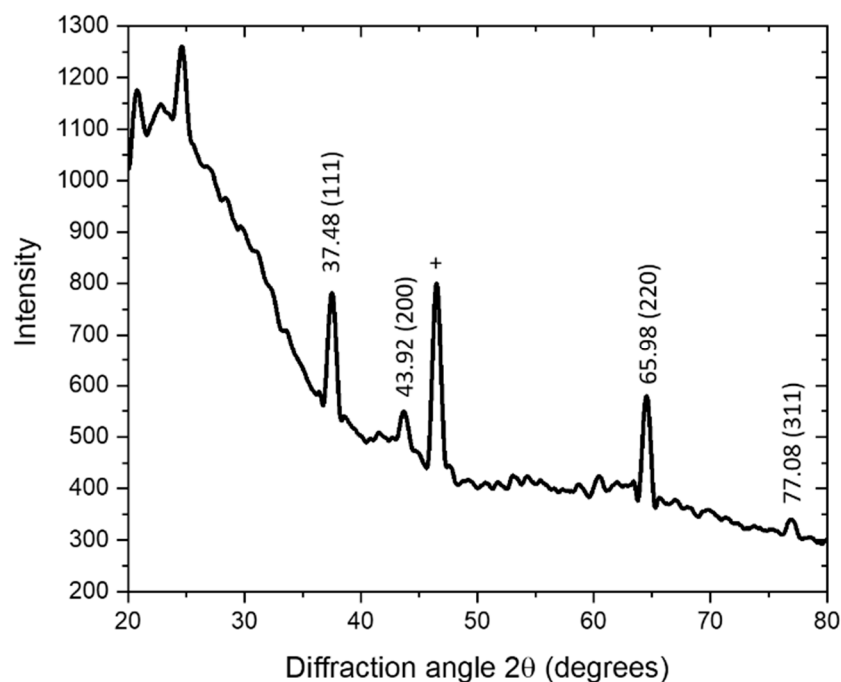


**Figure 4.** The XRD spectrum of green AgNPs, synthesized using *B. flexuosa* leave extract. The samples were scanned in the range of  $0^\circ$  to  $80^\circ$  at a diffraction angle of  $2\theta$ , with an Ultima IV X-ray diffractometer (Rigaku, Japan) using cobalt radiation ( $\text{CuK}\alpha$ ), which had a voltage of 40 kV and a current of 30 mA at room temperature.

The synthesized AgNPs were investigated, using SEM, to characterize their size, shape, and morphology. The SEM image is shown in Figure 5, and shows colloidal and well-dispersed particles.

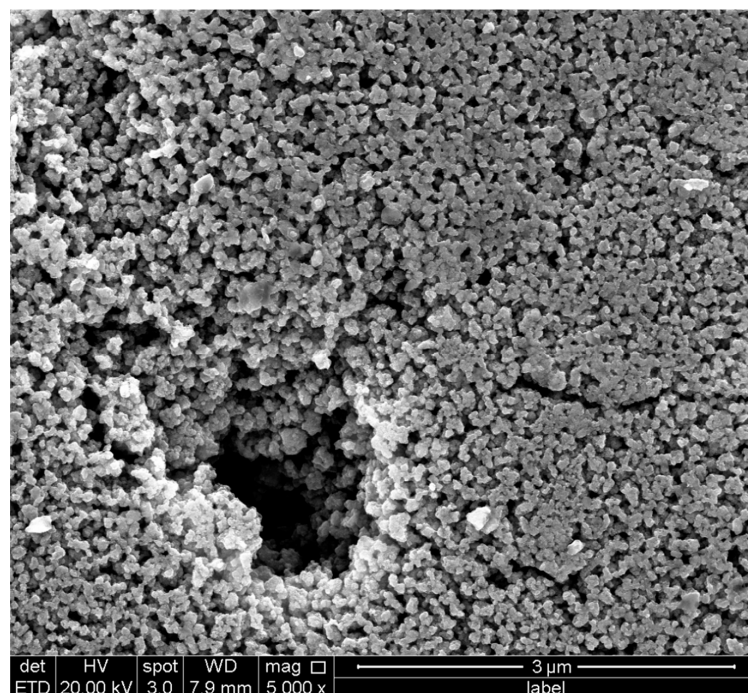


**Figure 5.** The SEM image of the synthesized SEM ((Model QUANTA FEG 450, FEI, Thermo Fisher Scientific, Darmstadt, Germany).

### 3.2. Antimicrobial Activity of the AgNPs

The sensitivity of the tested bacteria to the prepared AgNPs was assessed by determining the OD data from the bacterial broth that contained the NPs at a concentration of 150 µg/mL. Rajasekar et al. tested the antibacterial activity of the produced AgNPs, which showed dose-dependent, and bacterial inhibition was observed at 150 µg/mL [51]. In addition, other reported work tested the AgNPs bacterial activity against *P. aeruginosa*, and *E. coli* showed strong inhibition at the selected concentration [52].

The ODs data for 24 h were obtained using a plate reader to measure the antimicrobial effect of the NPs. It was reported by other researchers that higher ODs values indicated higher bacterial growth [53,54]. The final OD was slightly lower in the broths that contained the AgNPs in comparison to the controls, which indicated that the prepared AgNPs had antimicrobial activity; it also demonstrated the good antibacterial effect of AgNPs on both Gram-negative and Gram-positive bacteria, without developing resistance. A systematic review paper by Rai et al. concluded that AgNPs have strong bactericidal activity against both Gram-positive and Gram-negative bacteria [55]; as they mentioned, and up to the year 2012, AgNPs showed activity against many strains, including *E. coli*, *V. cholerae*, *P. aeruginosa*, *Staph. aureus* and *S. typhus* [55]. However, the activity of AgNPs was much higher against Gram-positive bacteria—namely, *E. faecalis* and *S. epidermidi*—than against Gram-negative bacteria—namely, *P. aeruginosa*, *E. coli*, *K. pneumonia*, and *S. enterica*; Table 3 and Figure 6. Similar results were observed when AgNPs (prepared using *L. tuber* extract) were tested on *Gloriosa superba* and *E. faecalis*. The latter, which is a Gram-positive bacteria, was more sensitive to the NPs [56]. This was explained by the fact that the AgNPs carried positive charges that interacted with the negatively charged bacterial cell walls, adhered, and penetrated the bacterial cell, leading to the loss of cell wall integrity and permeability [57]. It is known that Gram-positive bacteria carry a negative charge on their cell wall, because of the presence of teichoic acids linked to either the peptidoglycan or to the underlying plasma membrane; whereas, in Gram-negative bacteria, the negative charge has a lower impact—in comparison to Gram-positive bacteria—because of their outer covering, that is made of phospholipids and lipopolysaccharides [58].

**Table 3.** The ODs results for *P. aeruginosa*, *E. coli*, *K. pneumonia*, *S. enterica*, *E. faecalis*, and *S. epidermidis*, after 24 h of incubating at 37 °C with the freshly prepared AgNPs and the negative control; without AgNPs. The quantification of the total number of bacteria was done in triplicate.

Bacterial Strain	Negative Control	AgNPs
<i>P. aeruginosa</i> (0.174)	1.665 ± 0.029	1.491 ± 0.033
<i>E. coli</i> (0.272)	2.040 ± 0.031	1.768 ± 0.027
<i>K. pneumonia</i> (0.26)	2.012 ± 0.001	1.752 ± 0.030
<i>S. enterica</i> (0.303)	1.897 ± 0.047	1.594 ± 0.014
<i>E. faecalis</i> (0.7)	1.879 ± 0.0502	1.113 ± 0.055
<i>S. epidermidis</i> (0.33)	1.917 ± 0.011	1.587 ± 0.012

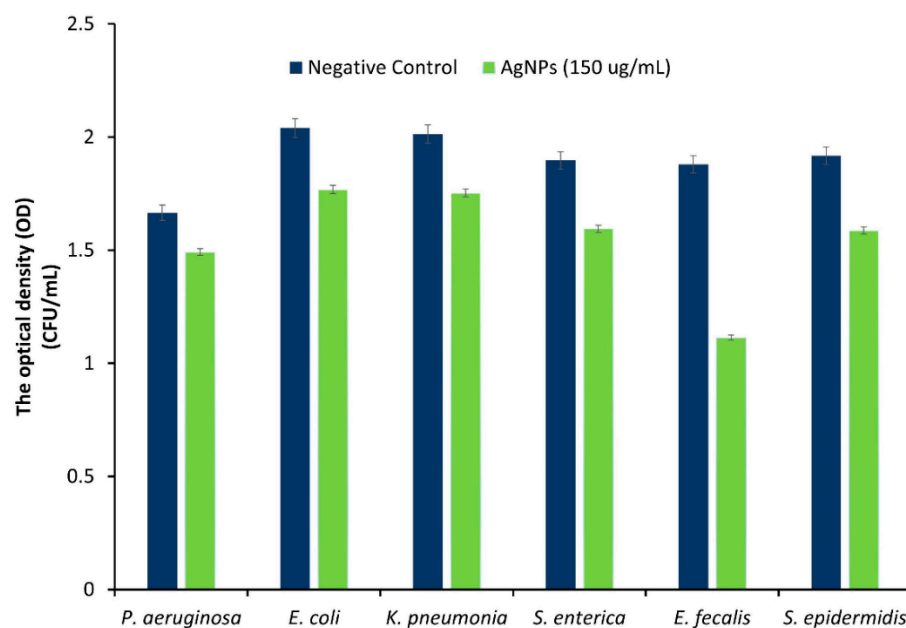


**Figure 6.** The ODs data for 150 µg/mL of AgNPs against *P. aeruginosa*, *E. coli*, *K. pneumonia*, *S. enterica*, *E. fecalis*, and *S. epidermidis*, after 24 h of incubating at 37 °C. The quantification of the total number of bacteria was done in triplicate.

#### 4. Conclusions

In this work, *B. flexuosa* methanolic leaf extract was used for the first time to prepare AgNPs. The formation and the properties of the NPs were affected by the experimental conditions. For instance, the particles were not formed in neutral or acidic media, while they were formed, and their stability was enhanced as the pH increased. Furthermore, the size and the charge of the NPs increased as the concentration of the precursor (AgNO<sub>3</sub>) increased. On the other hand, the uniformity of the particles increased as the concentration of AgNO<sub>3</sub> decreased. Finally, the selected NPs showed activity against the studied strains of both Gram-positive and Gram-negative bacteria, but with better activity on the Gram-positive strains. Based on this work, we believe that the *B. flexuosa* methanolic leaf extract can be used in the future to prepare AgNPs. The green method mentioned herein, to prepare AgNPs, is expected to be economic, eco-friendly, and effective in preparing a wide-spectrum antimicrobial agent. First of all, however, further studies are needed, such as optimizing the formulation, and performing in vivo studies.

**Author Contributions:** Conceptualization, N.A.-N.; methodology, N.A.-N., F.H. and T.E.-E.; validation, N.A.-N., F.H. and T.E.-E.; formal analysis, N.A.-N., F.H. and T.E.-E.; investigation, N.A.-N. and F.H.; resources, N.A.-N. and T.E.-E.; data curation, F.H.; writing—original draft preparation, N.A.-N., F.H. and T.E.-E.; writing—review and editing, N.A.-N., F.H. and T.E.-E.; visualization, N.A.-N. and F.H.; supervision, N.A.-N. and T.E.-E.; project administration, N.A.-N.; funding acquisition, N.A.-N. All authors have read and agreed to the published version of the manuscript.

**Funding:** The authors thank the Deanship of Research at Jordan University of Science and Technology (JUST) for their generous fund (Proposal Number: 20210257).

**Conflicts of Interest:** The authors declare no conflict of interest.

## References

1. Mody, V.; Siwale, R.; Singh, A.; Mody, H. Introduction to metallic nanoparticles. *J. Pharm. Bioallied Sci.* **2010**, *2*, 282. [[CrossRef](#)] [[PubMed](#)]
2. Singla, R.; Guliani, A.; Kumari, A.; Yadav, S.K. Metallic nanoparticles, toxicity issues and applications in medicine. In *Nanoscale Materials in Targeted Drug Delivery, Theragnosis and Tissue Regeneration*; Springer: Singapore, 2016; pp. 41–80. [[CrossRef](#)]
3. Ahmad, M.Z.; Akhter, S.; Jain, G.K.; Rahman, M.; Pathan, S.A.; Ahmad, F.J.; Khar, R.K. Metallic nanoparticles: Technology overview & drug delivery applications in oncology. *Expert Opin. Drug Deliv.* **2010**, *7*, 927–942. [[CrossRef](#)] [[PubMed](#)]
4. Kumar, H.; Venkatesh, N.; Bhowmik, H.; Kuila, A. Metallic Nanoparticle: A Review. *Biomed. J. Sci. Tech. Res.* **2018**, *4*, 3765–3775. [[CrossRef](#)]
5. Mandava, K. Biological and Non-biological Synthesis of Metallic Nanoparticles: Scope for Current Pharmaceutical Research. *Indian J. Pharm. Sci.* **2017**, *79*, 501–512. [[CrossRef](#)]
6. Mohanty, S.; Mishra, S.; Jena, P.; Jacob, B.; Sarkar, B.; Sonawane, A. An investigation on the antibacterial, cytotoxic, and antibiofilm efficacy of starch-stabilized silver nanoparticles. *Nanomed. Nanotechnol. Biol. Med.* **2012**, *8*, 916–924. [[CrossRef](#)]
7. Shaikh, S.; Nazam, N.; Rizvi, S.M.D.; Ahmad, K.; Baig, M.H.; Lee, E.J.; Choi, I. Mechanistic Insights into the Antimicrobial Actions of Metallic Nanoparticles and Their Implications for Multidrug Resistance. *Int. J. Mol. Sci.* **2019**, *20*, 2468. [[CrossRef](#)]
8. Kumar, V.S.; Nagaraja, B.M.; Shashikala, V.; Padmasri, A.H.; Madhavendra, S.S.; Raju, B.D.; Rao, K.S.R. Highly efficient Ag/C catalyst prepared by electro-chemical deposition method in controlling microorganisms in water. *J. Mol. Catal. A Chem.* **2004**, *223*, 313–319. [[CrossRef](#)]
9. Ahmed, S.; Ahmad, M.; Swami, B.L.; Ikram, S. A review on plants extract mediated synthesis of silver nanoparticles for antimicrobial applications: A green expertise. *J. Adv. Res.* **2016**, *7*, 17–28. [[CrossRef](#)]
10. Echegoyen, Y.; Nerín, C. Nanoparticle release from nano-silver antimicrobial food containers. *Food Chem. Toxicol.* **2013**, *62*, 16–22. [[CrossRef](#)]
11. Rai, M.; Yadav, A.; Gade, A. Silver nanoparticles as a new generation of antimicrobials. *Biotechnol. Adv.* **2009**, *27*, 76–83. [[CrossRef](#)]
12. Teirumnieks, E.; Balchev, I.; Ghalot, R.S.; Lazov, L. Antibacterial and anti-viral effects of silver nanoparticles in medicine against COVID-19—A review. *Laser Phys.* **2021**, *31*, 013001. [[CrossRef](#)]
13. Sun, Y.; Yin, Y.; Mayers, B.T.; Herricks, T.; Xia, Y. Uniform silver nanowires synthesis by reducing AgNO<sub>3</sub> with ethylene glycol in the presence of seeds and poly(vinyl pyrrolidone). *Chem. Mater.* **2002**, *14*, 4736–4745. [[CrossRef](#)]
14. Callegari, A.; Tonti, D.; Chergui, M. Photochemically Grown Silver Nanoparticles with Wavelength-Controlled Size and Shape. *Nano Lett.* **2003**, *3*, 1565–1568. [[CrossRef](#)]
15. Dimitrijevic, N.M.; Bartels, D.M.; Jonah, C.D.; Takahashi, K.; Rajh, T. Radiolytically induced formation and optical absorption spectra of colloidal silver nanoparticles in supercritical ethane. *J. Phys. Chem. B* **2001**, *105*, 954–959. [[CrossRef](#)]
16. Swami, A.; Selvakannan, P.R.; Pasricha, R.; Sastry, M. One-step synthesis of ordered two-dimensional assemblies of silver nanoparticles by the spontaneous reduction of silver ions by pentadecylphenol langmuir monolayers. *J. Phys. Chem. B* **2004**, *108*, 19269–19275. [[CrossRef](#)]
17. Joseph, S.; Mathew, B. Microwave assisted facile green synthesis of silver and gold nanocatalysts using the leaf extract of *Aerva lanata*. *Spectrochim. Acta Part A Mol. Biomol. Spectrosc.* **2015**, *136*, 1371–1379. [[CrossRef](#)]
18. Abid, J.P.; Wark, A.W.; Brevet, P.F.; Girault, H.H. Preparation of silver nanoparticles in solution from a silver salt by laser irradiation. *Chem. Commun.* **2002**, *7*, 792–793. [[CrossRef](#)]
19. Naik, R.R.; Stringer, S.J.; Agarwal, G.; Jones, S.E.; Stone, M.O. Biomimetic synthesis and patterning of silver nanoparticles. *Nat. Mater.* **2002**, *1*, 169–172. [[CrossRef](#)]
20. Ahmad, A.; Mukherjee, P.; Senapati, S.; Mandal, D.; Khan, M.I.; Kumar, R.; Sastry, M. Extracellular biosynthesis of silver nanoparticles using the fungus *Fusarium oxysporum*. *Colloids Surfaces B Biointerfaces* **2003**, *28*, 313–318. [[CrossRef](#)]
21. Shah, M.; Fawcett, D.; Sharma, S.; Tripathy, S.K.; Poinern, G.E.J. Green Synthesis of Metallic Nanoparticles via Biological Entities. *Materials* **2015**, *8*, 7278–7308. [[CrossRef](#)]
22. Gardea-Torresdey, J.L.; Gomez, E.; Peralta-Videa, J.R.; Parsons, J.G.; Troiani, H.; Jose-Yacaman, M. Alfalfa Sprouts: A Natural Source for the Synthesis of Silver Nanoparticles. *Langmuir* **2003**, *19*, 1357–1361. [[CrossRef](#)]
23. Salem, S.S.; Fouda, A. Green Synthesis of Metallic Nanoparticles and Their Prospective Biotechnological Applications: An Overview. *Biol. Trace Elem. Res.* **2021**, *199*, 344–370. [[CrossRef](#)] [[PubMed](#)]
24. Rahim, M.; Rizvi, S.M.D.; Iram, S.; Khan, S.; Bagga, P.S.; Khan, M.S. Interaction of green nanoparticles with cells and organs. In *Inorganic Frameworks as Smart Nanomedicines*; William Andrew Publishing: Norwich, NY, USA, 2018; pp. 185–237. [[CrossRef](#)]
25. Mariselvam, R.; Ranjitsingh, A.J.A.; Usha Raja Nanthini, A.; Kalirajan, K.; Padmalatha, C.; Mosae Selvakumar, P. Green synthesis of silver nanoparticles from the extract of the inflorescence of *Cocos nucifera* (Family: Arecaceae) for enhanced antibacterial activity. *Spectrochim. Acta Part A Mol. Biomol. Spectrosc.* **2014**, *129*, 537–541. [[CrossRef](#)]
26. Krishnaraj, C.; Jagan, E.G.; Rajasekar, S.; Selvakumar, P.; Kalaichelvan, P.T.; Mohan, N. Synthesis of silver nanoparticles using *Acalypha indica* leaf extracts and its antibacterial activity against water borne pathogens. *Colloids Surf. B Biointerfaces* **2010**, *76*, 50–56. [[CrossRef](#)] [[PubMed](#)]
27. Taifour, H. Jordan Plant Red List. In Proceedings of the Royal Botanic Garden 1st Annual Scientific Day, Amman, Jordan, 12 January 2012; Royal Botanic Garden 1st Annual Scientific Day: Amman, Jordan, 2012.

28. El-Elimat, T.; Rivera-Chávez, J.; Burdette, J.E.; Czarnecki, A.; Alhawarri, M.B.; Al-Gharaibeh, M.; Alali, F.; Oberlies, N.H. Cytotoxic homoisoflavonoids from the bulbs of *Bellevalia flexuosa*. *Fitoterapia* **2018**, *127*, 201–206. [[CrossRef](#)]
29. Lin, L.-G.; Liu, Q.-Y.; Ye, Y. Naturally Occurring Homoisoflavonoids and Their Pharmacological Activities. *Planta Med.* **2014**, *80*, 1053–1066. [[CrossRef](#)]
30. Rashidipour, M.; Heydari, R. Biosynthesis of silver nanoparticles using extract of olive leaf: Synthesis and in vitro cytotoxic effect on MCF-7 cells. *J. Nanostructure Chem.* **2014**, *4*, 112. [[CrossRef](#)]
31. Chang, Y.C.; Yang, C.Y.; Sun, R.L.; Cheng, Y.F.; Kao, W.C.; Yang, P.C. Rapid single cell detection of *Staphylococcus aureus* by aptamer-conjugated gold nanoparticles. *Sci. Rep.* **2013**, *3*, 1863. [[CrossRef](#)]
32. Luna-Sánchez, J.L.; Jiménez-Pérez, J.L.; Carbajal-Valdez, R.; Lopez-Gamboa, G.; Pérez-González, M.; Correa-Pacheco, Z.N. Green synthesis of silver nanoparticles using Jalapeño Chili extract and thermal lens study of acrylic resin nanocomposites. *Thermochim. Acta* **2019**, *678*, 178314. [[CrossRef](#)]
33. Salehi, S.; Sadat Shandiz, S.A.; Ghanbar, F.; Darvish, M.R.; Ardestani, M.S.; Mirzaie, A.; Jafari, M. Phytosynthesis of silver nanoparticles using *Artemisia marschalliana* Sprengel aerial part extract and assessment of their antioxidant, anticancer, and antibacterial properties. *Int. J. Nanomed.* **2016**, *11*, 1835–1846. [[CrossRef](#)]
34. Anigol, L.B.; Balekundri, S.G.; Charantimath, J.S.; Gurubasavaraj, P.M. Effect of Concentration and pH on the Size of Silver Nanoparticles Synthesized by Green Chemistry. *Org. Med. Chem.* **2017**, *3*, 124–128. [[CrossRef](#)]
35. Dehnavi, A.S.; Raisi, A.; Aroujalian, A. Control Size and Stability of Colloidal Silver Nanoparticles with Antibacterial Activity Prepared by a Green Synthesis Method. *Synth. React. Inorg. Met. Nano-Metal Chem.* **2013**, *43*, 543–551. [[CrossRef](#)]
36. Chutrakulwong, F.; Thamaphat, K.; Limsuwan, P. Photo-irradiation induced green synthesis of highly stable silver nanoparticles using durian rind biomass: Effects of light intensity, exposure time and pH on silver nanoparticles formation. *J. Phys. Commun.* **2020**, *4*, 095015. [[CrossRef](#)]
37. Dadashpour, M.; Firouzi-Amandi, A.; Pourhassan-Moghaddam, M.; Maleki, M.J.; Soozangar, N.; Jeddi, F.; Nouri, M.; Zarghami, N.; Pilehvar-Soltanahmadi, Y. Biomimetic synthesis of silver nanoparticles using *Matricaria chamomilla* extract and their potential anticancer activity against human lung cancer cells. *Mater. Sci. Eng. C. Mater. Biol. Appl.* **2018**, *92*, 902–912. [[CrossRef](#)] [[PubMed](#)]
38. Razavi, R.; Amiri, M.; Alshamsi, H.A.; Eslaminejad, T.; Salavati-Niasari, M. Green synthesis of Ag nanoparticles in oil-in-water nano-emulsion and evaluation of their antibacterial and cytotoxic properties as well as molecular docking. *Arab. J. Chem.* **2021**, *14*, 103323. [[CrossRef](#)]
39. Sánchez, G.R.; Castilla, C.L.; Gómez, N.B.; García, A.; Marcos, R.; Carmona, E.R. Leaf extract from the endemic plant *Peumus boldus* as an effective bioproduct for the green synthesis of silver nanoparticles. *Mater. Lett.* **2016**, *183*, 255–260. [[CrossRef](#)]
40. Elzey, S.; Grassian, V.H. Agglomeration, isolation and dissolution of commercially manufactured silver nanoparticles in aqueous environments. *J. Nanoparticle Res.* **2010**, *12*, 1945–1958. [[CrossRef](#)]
41. Kumar, P.; Govindaraju, M.; Senthamselvi, S.; Premkumar, K. Photocatalytic degradation of methyl orange dye using silver (Ag) nanoparticles synthesized from *Ulva lactuca*. *Colloids Surf. B. Biointerfaces* **2013**, *103*, 658–661. [[CrossRef](#)] [[PubMed](#)]
42. Wang, M.; Li, H.; Li, Y.; Mo, F.; Li, Z.; Chai, R.; Wang, H. Dispersibility and Size Control of Silver Nanoparticles with Anti-Algal Potential Based on Coupling Effects of Polyvinylpyrrolidone and Sodium Tripolyphosphate. *Nanomater* **2020**, *10*, 1042. [[CrossRef](#)]
43. Danaei, M.; Dehghankhold, M.; Ataei, S.; Hasanzadeh Davarani, F.; Javanmard, R.; Dokhani, A.; Khorasani, S.; Mozafari, M.R. Impact of Particle Size and Polydispersity Index on the Clinical Applications of Lipidic Nanocarrier Systems. *Pharmaceutics* **2018**, *10*, 57. [[CrossRef](#)] [[PubMed](#)]
44. Demeler, B.; Nguyen, T.L.; Gorbet, G.E.; Schirf, V.; Brookes, E.H.; Mulvaney, P.; El-Ballouli, A.O.; Pan, J.; Bakr, O.M.; Demeler, A.K.; et al. Characterization of size, anisotropy, and density heterogeneity of nanoparticles by sedimentation velocity. *Anal. Chem.* **2014**, *86*, 7688–7695. [[CrossRef](#)]
45. Chorny, M.; Fishbein, I.; Danenberg, H.D.; Golomb, G. Lipophilic drug loaded nanospheres prepared by nanoprecipitation: Effect of formulation variables on size, drug recovery and release kinetics. *J. Control. Release* **2002**, *83*, 389–400. [[CrossRef](#)]
46. Cakić, M.; Glišić, S.; Cvetković, D.; Cvetinov, M.; Stanojević, L.; Danilović, B.; Cakić, K. Green Synthesis, Characterization and Antimicrobial Activity of Silver Nanoparticles Produced from *Fumaria officinalis* L. Plant Extract. *Colloid J.* **2018**, *80*, 803–813. [[CrossRef](#)]
47. Marshall, A.T.; Haverkamp, R.G.; Davies, C.E.; Parsons, J.G.; Gardea-Torresdey, J.L.; van Agterveld, D. Accumulation of Gold Nanoparticles in Brassic Juncea. *Int. J. Phytoremediation* **2007**, *9*, 197–206. [[CrossRef](#)]
48. Ahmad, N.; Sharma, S. Green Synthesis of Silver Nanoparticles Using Extracts of *Ananas comosus*. *Green Sustain. Chem.* **2012**, *2*, 141–147. [[CrossRef](#)]
49. Christy, A.J.; Umadevi, M. Synthesis and characterization of monodispersed silver nanoparticles. *Adv. Nat. Sci. Nanosci. Nanotechnol.* **2012**, *3*, 035013. [[CrossRef](#)]
50. Khatami, M.; Sharifi, I.; Nobre, M.A.L.; Zafarnia, N.; Aflatoonian, M.R. Waste-grass-mediated green synthesis of silver nanoparticles and evaluation of their anticancer, antifungal and antibacterial activity. *Green Chem. Lett. Rev.* **2018**, *11*, 125–134. [[CrossRef](#)]
51. Rajasekar, P.; Palanisamy, S.; Anjali, R.; Vinosha, M.; Thillaiaswari, M.; Malaikozhundan, B.; Boomi, P.; Saravanan, M.; You, S.G.; Prabhu, N.M. *Cladophora fascicularis* Mediated Silver Nanoparticles: Assessment of Their Antibacterial Activity Against *Aeromonas hydrophila*. *J. Clust. Sci.* **2020**, *31*, 673–683. [[CrossRef](#)]

52. Lateef, A.; Azeez, M.A.; Asafa, T.B.; Yekeen, T.A.; Akinboro, A.; Oladipo, I.C.; Azeez, L.; Ajibade, S.E.; Ojo, S.A.; Gueguim-Kana, E.B.; et al. Biogenic synthesis of silver nanoparticles using a pod extract of *Cola nitida*: Antibacterial and antioxidant activities and application as a paint additive. *J. Taibah Univ. Sci.* **2016**, *10*, 551–562. [[CrossRef](#)]
53. Rutherford, D.; Jíra, J.; Kolářová, K.; Matolínová, I.; Mičová, J.; Remeš, Z.; Rezek, B. Growth Inhibition of Gram-Positive and Gram-Negative Bacteria by Zinc Oxide Hedgehog Particles. *Int. J. Nanomed.* **2021**, *16*, 3541. [[CrossRef](#)] [[PubMed](#)]
54. Alshareef, A.; Laird, K.; Cross, R.B.M. Shape-dependent antibacterial activity of silver nanoparticles on *Escherichia coli* and *Enterococcus faecium* bacterium. *Appl. Surf. Sci.* **2017**, *424*, 310–315. [[CrossRef](#)]
55. Rai, M.K.; Deshmukh, S.D.; Ingle, A.P.; Gade, A.K. Silver nanoparticles: The powerful nanoweapon against multidrug-resistant bacteria. *J. Appl. Microbiol.* **2012**, *112*, 841–852. [[CrossRef](#)]
56. Murugesan, A.K.; Pannerselvam, B.; Javee, A.; Rajenderan, M.; Thiyagarajan, D. Facile green synthesis and characterization of *Gloriosa superba* L. tuber extract-capped silver nanoparticles (GST-AgNPs) and its potential antibacterial and anticancer activities against A549 human cancer cells. *Environ. Nanotechnol. Monit. Manag.* **2021**, *15*, 100460. [[CrossRef](#)]
57. Morones, J.R.; Elechiguerra, J.L.; Camacho, A.; Holt, K.; Kouri, J.B.; Ramírez, J.T.; Yacaman, M.J. The bactericidal effect of silver nanoparticles. *Nanotechnology* **2005**, *16*, 2346–2353. [[CrossRef](#)] [[PubMed](#)]
58. Guzman, M.; Dille, J.; Godet, S. Synthesis and antibacterial activity of silver nanoparticles against gram-positive and gram-negative bacteria. *Nanomedicine* **2012**, *8*, 37–45. [[CrossRef](#)] [[PubMed](#)]